Optimal Laser Scan Path for Localizing a Fluorescent Particle in Two or Three Dimensions

Gregg M. Gallatin and Andrew J. Berglund

Center for Nanoscale Science and Technology
National Institute of Standards and Technology
Gaithersburg, MD 20899, USA

gregg.gallatin@nist.gov

Abstract: Localizing a fluorescent particle by scanning a focused laser beam in its vicinity and analyzing the detected photon stream provides real-time information for a modern class of feedback control systems for particle tracking and trapping. We show for the full range of standard merit functions based on the Fisher information matrix (1) that the optimal path coincides with the positions of maximum slope of the square root of the beam intensity rather than with the intensity itself, (2) that this condition matches that derived from the theory describing the optimal design of experiments and (3) that in one dimension it is equivalent to maximizing the signal to noise ratio. The optimal path for a Gaussian beam scanned in two or three dimensions is presented along with the Cramér-Rao bound, which gives the ultimate localization accuracy that can be achieved by analyzing the detected photon stream. In two dimensions the optimum path is independent of the chosen merit function but this is not the case in three dimensions. Also, we show that whereas the optimum path for a Gaussian beam in two dimensions can be chosen to be continuous, it cannot be continuous in three dimensions.

OCIS codes: (180.2520) Fluorescence Microscopy; (110.3055) Imaging systems, information theoretical analysis.

References and links

1. R. Thompson, D. Larson, and W. Webb, "Precise Nanometer Localization Analysis for Individual Fluorescent Probes," Biophys. J. **82**(5), 2775–2783 (2002).
2. R. Ober, S. Ram, and E. Ward, "Localization accuracy in single-molecule microscopy," Biophys. J. **86**(2), 1185–1200 (2004).
3. M. Cheezum, W. Walker, and W. Guilford, "Quantitative Comparison of Algorithms for Tracking Single Fluorescent Particles," Biophys. J. **81**(4), 2378–2388 (2001).
4. J. Crocker and D. Grier, "Methods of Digital Video Microscopy for Colloidal Studies," J. Colloid Interface Sci. **179**(1), 298–310 (1996).
5. T. Savin and P. S. Doyle, "Static and Dynamic Errors in Particle Tracking Microrheology," Biophys. J. **88**, 623–638 (2005).
6. M. Dahan, S. Levi, C. Luccardini, P. Rostaing, B. Riveau, and A. Triller, "Diffusion Dynamics of Single Glycine Receptors Revealed by Single-Quantum Dot Tracking," Science **302**, 442–445 (2003).
7. A. Yildiz, J. N. Forkey, S. A. McKinney, T. Ha, Y. E. Goodman, and P. R. Selvin, "Myosin V walks hand-over-hand: Single fluorophore imaging with 1.5-nm localization," Science **300**, 2061–2065 (2003).
8. B. Huang, M. Bates, and X. Zhuang, "Super resolution fluorescence microscopy," Annu. Rev. Biochem. **78**, 993–1016 (2010).

9. W. E. Moerner, "New directions in single-molecule imaging and analysis," Proc. Natl. Acad. Sci. USA **104**, 12,596–12,602 (2007).
10. H. Cang, C. Shan Xu, and H. Yang, "Progress in single-molecule tracking spectroscopy," Chemical Physics Letters **457**(4-6), 285–291 (2008).
11. A. P. Fields and A. E. Cohen, "Anti-Brownian traps for studies on single molecules," Methods in enzymology **475**, 149–174 (2010).
12. M. Armani, S. Chaudhary, R. Probst, and B. Shapiro, "Using feedback control and micro-fluidics to steer individual particles," Micro Electro Mechanical Systems, 2005. MEMS 2005. 18th IEEE International Conference on pp. 855–858.
13. A. J. Berglund and H. Mabuchi, "Tracking-FCS: Fluorescence Correlation Spectroscopy of Individual Particles," Opt. Express **13**, 8069–8082 (2005).
14. A. E. Cohen and W. E. Moerner, "Method for Trapping and Manipulating Nanoscale Objects in Solution," Appl. Phys. Lett. **86**(9), 093,109 (2005).
15. M. Armani, S. Chaudhary, R. Probst, and B. Shapiro, "Using feedback control of microflows to independently steer multiple particles," IEEE J. Microelectromech. Syst. **15**(4), 945–956 (2006).
16. A. E. Cohen and W. E. Moerner, "Suppressing Brownian Motion of Individual Biomolecules in Solution," Proc. Natl. Acad. Sci. USA **103**, 4362–4365 (2006).
17. Z. Shen and S. Andersson, "Tracking Nanometer-Scale Fluorescent Particles in Two Dimensions With a Confocal Microscope," Control Systems Technology, IEEE Transactions on (99), 1–10 (2010).
18. A. P. Fields and A. E. Cohen, "Electrokinetic trapping at the one nanometer limit," Proceedings of the National Academy of Sciences **108**(22), 8937 (2011).
19. V. Levi, Q. Ruan, K. Kis-Petikova, and E. Gratton, "Scanning FCS, a Novel Method for Three-Dimensional Particle Tracking," Biochem. Soc. Trans. **31**, 997–1000 (2003).
20. V. Levi, Q. Ruan, and E. Gratton, "3-D particle tracking in a two-photon microscope. Application to the study of molecular dynamics in cells," Biophys. J. **88**, 2919–2928 (2005).
21. H. Cang, C. M. Wong, C. S. Xu, A. H. Rizvi, and H. Yang, "Confocal three dimensional tracking of a single nanoparticle with concurrent spectroscopic readout," Appl. Phys. Lett. **88**, 223,901 (2006).
22. K. McHale, A. J. Berglund, and H. Mabuchi, "Quantum dot photon statistics measured by three-dimensional particle tracking," Nano Letters **7**, 3535–3539 (2007).
23. G. Lessard, P. Goodwin, and J. Werner, "Three-dimensional tracking of individual quantum dots," Appl. Phys. Lett. **91**, 224,106 (2007).
24. H. Cang, D. Montiel, C. Xu, and H. Yang, "Observation of spectral anisotropy of gold nanoparticles," The Journal of chemical physics **129**, 044,503 (2008).
25. K. McHale and H. Mabuchi, "Precise characterization of the conformation fluctuations of freely diffusing DNA: beyond Rouse and Zimm," Journal of the American Chemical Society **131**(49), 17,901–17,907 (2009).
26. A. J. Berglund and H. Mabuchi, "Performance Bounds on Single-Particle Tracking by Fluorescence Modulation," Appl. Phys. B **83**, 127–133 (2006).
27. A. J. Berglund, K. McHale, and H. Mabuchi, "Feedback Localization of Freely Diffusing Fluorescent Particles Near the Optical Shot-Noise Limit," Opt. Lett. **32**, 145–147 (2007).
28. Z. Shen and S. Andersson, "Optimal measurement constellation of the fluoroBancroft localization algorithm for position estimation in tracking confocal microscopy," Mechatronics (2011).
29. Q. Wang and W. Moerner, "Optimal strategy for trapping single fluorescent molecules in solution using the ABEL trap," Applied Physics B: Lasers and Optics **99**(1), 23–30 (2010).
30. A. E. Siegman, *Lasers* (University Science Books, 1986).
31. H. Kao and A. Verkman, "Tracking of single fluorescent particles in three dimensions: use of cylindrical optics to encode particle position," Biophys. J. **67**, 1291–1300 (1994).
32. S. Pavani and R. Piestun, "Three dimensional tracking of fluorescent microparticles using a photon-limited double-helix response system," Opt. Express **16**, 22,048–22,057 (2008).
33. K. T. Seale, R. S. Reiserer, D. A. Markov, I. A. Ges, C. Wright, C. Janetopoulos, and J. P. Wikswo, "Mirrored pyramidal wells for simultaneous multiple vantage point microscopy," J. Microsc. **232**, 1–6 (2008).
34. M. D. McMahon, A. J. Berglund, P. Carmichael, J. J. McClelland, and J. A. Liddle, "3D Particle Trajectories Observed by Orthogonal Tracking Microscopy," ACS Nano **3**, 609–614 (2009).
35. S. Zacks, *The Theory of Statistical Inference* (John Wiley & Sons, 1971).
36. F. Pukelsheim, *Optimal design of experiments* (Society for Industrial and Applied Mathematics, 2006).

1. Introduction

We address the general problem of determining the position of a fluorescent particle by scanning a focused laser beam in its vicinity (see Fig. 1) and detecting, on a single-pixel (i.e. non-imaging) detector such as a single-photon counter, the fluorescent photons generated by the particle. This method provides a modern, real-time alternative to image-based single-particle

localization in optical microscopy [1–3] - which has been widely applied for studying colloidal and biophysical systems [4–7] and achieving nanometer-scale "super-resolution" single-molecule images [8] - and is critical to a new class of measurement technique [9–11] wherein a single fluorescent particle is located in real time while a feedback controller tracks or traps the particle to maintain its position in the observation volume of a microscope. Each experimental implementation uses a different combination of laser scanning or multiple detector placement, sample scanning, and localization algorithm to accomplish a real-time position measurement in two [12–18] or three [19–25] dimensions. While the referenced experimental implementations have each been used successfully, *optimal* strategies have been identified only for restricted cases of the laser scan pattern or estimation algorithm: under a Gaussian noise approximation the optimal circular scan path for two-dimensional localization was found in Ref. [26,27]; under a Gaussian noise approximation and for a particular estimator - the fluoroBancroft algorithm - an optimal three-dimensional laser scan path was found in [28]; a complex two-dimensional scan geometry was studied in Ref. [29] for the case of a particle that cannot be localized within the "linear" estimator range of the focused beam. To date, however, neither a unified, global optimality strategy has not been identified nor have the fundamental limits to localization accuracy been established. We solve this problem here. We show that for the full range of standard scalar merit functions that can be defined using the Fisher information matrix the optimum trajectory is consistent with maintaining the particle at the positions of maximum slope of the square root of the intensity rather than at the maximum slope of the intensity itself but that the optimum time spent at these positions does depend on the particular choice of merit function. We also discuss how this is related to maximizing the signal to noise. For Gaussian beams we show that these results exactly match those that can be derived from the theory of the optimal design of experiments. Based on these results we introduce a simple test that can be applied to determine the degree of optimality of any experimental design with mathematical rigor. This test allows a user to ascertain quickly whether a particular laser scan path (in two or three dimensions) provides maximum information about a particle's position for a particular focused-beam geometry. These results hold under the assumption that the particle is effectively stationary during the scan period which does not necessarily suffice for the situation studied in Ref. [29], where the beam is scanned over a relatively large range to accommodate a very fast moving particle. A more general and difficult problem, not addressed here, is to devise a strategy for locating a particle that explores a significant fraction of the excitation geometry *during the scan time*. Under this quasi-stationary assumption we solve the optimal scan path problem completely.

Specifically we find that for a Gaussian beam in two dimensions (2D) the fundamental bounds on the localization accuracy are

$$\sigma_x^2 + \sigma_y^2 \geq \frac{w_0^2}{2N_{ph}} \tag{1}$$

where σ_k is the standard deviation in position measured along $k \in \{x,y,z\}$, w_0 is the focused Gaussian beam waist [30] and N_{ph} the (average) number of photons collected during the scan time. Note that Eq. 1 is identical to the standard image-based result when a Gaussian point-spread function is assumed [1, 2], demonstrating the equivalent information content of a diffraction-limited image and the photon stream from an appropriately scanned diffraction-limited excitation beam.

For a Gaussian beam in three dimensions (3D) we find that for one particular choice of optimization function

$$\sigma_x^2 + \sigma_y^2 + \sigma_z^2 \geq \frac{w_0^2}{N_{ph}} \left(0.5 + 4.92\frac{w_0}{\lambda} + 11.10\frac{w_0^2}{\lambda^2} \right). \tag{2}$$

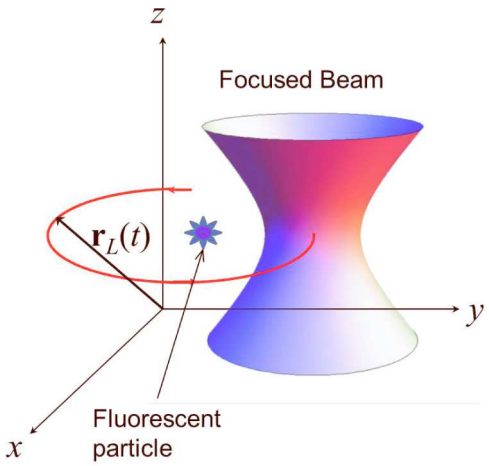

Fig. 1. Schematic diagram of a laser-scanning particle localization experiment. A Gaussian beam is scanned along a time-dependent (continuous or discrete) path $\mathbf{r}_L(t)$ and a modulated stream of photons is detected. The optimal design problem is to determine which scan path encodes maximal information about a particles location in the detected photon stream.

where λ is is the wavelength. There is no equivalent result for image-based three-dimensional localization corresponding to Eq. 2, though competing image-based methods [31–34] can (and should) be evaluated and compared to the bound given above. Making the following Gaussian approximation to the focused Airy diffraction pattern, $w_0 \approx 0.4\lambda/\mathrm{NA}$, where $\mathrm{NA} = \sin[\theta_{\max}]$ with $\theta_{\max}$ being the maximum angle the light illuminating the sample makes with respect to the z axis, the three-dimensional localization accuracy becomes

$$\sigma_x^2 + \sigma_y^2 + \sigma_z^2 \geq \frac{\lambda^2}{N_{ph}^2 \mathrm{NA}} \left(0.08 + \frac{0.31}{\mathrm{NA}} + \frac{0.28}{\mathrm{NA}^2} \right). \tag{3}$$

The remainder of the paper is devoted to a derivation and discussion of these results. We specify the problem in terms of the Fisher information matrix, give global optimality conditions, and identify scan paths for the familiar Gaussian beam profiles in two- and three-dimensions. In Appendix A we justify the global optimality condition and in Appendix B we derive the linearized maximum likelihood estimator based on the detected photon stream and foreknowledge of the beam shape (gradients and curvatures of the intensity profile), which can be applied in experimental hardware for real-time localization.

2. Theory of Optimal Design of Experments

Consider a laser beam with a position dependent intensity distribution $I(\mathbf{r})$ where $\mathbf{r} = (r_1, r_2, r_3) = (x, y, z)$. When the beam intensity is shifted to position $\mathbf{r}_\mathrm{L}$ and a fluorescent particle, is located at position $\mathbf{r}$, the intensity at the particle position is $I(\mathbf{r} - \mathbf{r}_\mathrm{L})$ and so the (average) rate at which fluorescent photons are generated is given by $\xi I(\mathbf{r} - \mathbf{r}_\mathrm{L})$ where ξ is the fluorescence cross-section (area) of the particle. Letting $\Gamma = \xi I$ with I in units of (incident photons)/(area$\times$time) it follows that Γ has units of (fluorescent photons)/time. (Note: Although it is convenient to think of $\mathbf{r}_\mathrm{L}$ as the position of peak intensity or as the centroid of the beam, this is not necessary. The solution to the optimization problem will automatically take whatever position definition is used into account.) Now suppose the beam is *scanned* over a time-dependent path $\mathbf{r}_\mathrm{L}(t)$ for a time period τ. Our task is to determine which scan path encodes the most in-

formation about the fluorescent particles position $\mathbf{r}$ in the detected fluorescent photon arrival times; that is, which path enables the best unbiased estimate of $\mathbf{r}$?

Fluorescently generated photons obey a Poisson distribution, i.e., over an extremely short time interval Δt the probability for detecting n photons when the particle is at position $\mathbf{r}$ and the laser beam is at position $\mathbf{r}_{\mathrm{L}}(t)$ is given by $(\Gamma(\mathbf{r}-\mathbf{r}_{\mathrm{L}}(t))\Delta t)^n/n!\exp\left[-\Gamma(\mathbf{r}-\mathbf{r}_{\mathrm{L}}(t))\Delta t\right]$. Hence over a finite time $\tau = N\Delta t$ the statistical description of the measurement process is defined by the the probability $p(t_1,...,t_K|\mathbf{r})$ of observing the set of K unordered photon arrival times $\{t_1,...,t_K\}$ in the interval $t\in[0,\tau)$ with

$$p(t_1,\ldots,t_K|\mathbf{r}) = \frac{1}{K!}\prod_{k=1}^{K}\Gamma(\mathbf{r}-\mathbf{r}_{\mathrm{L}}(t_k))\exp\left[-\int_0^\tau dt\Gamma(\mathbf{r}-\mathbf{r}_{\mathrm{L}}(t))\right] \tag{4}$$

where the product over k is understood to be unity for $K=0$ and we have replaced $\sum_{i=1}^{N}\Delta t\Gamma(\mathbf{r}-\mathbf{r}_{\mathrm{L}}(n\Delta t))$ with $\int_0^\tau dt\Gamma(\mathbf{r}-\mathbf{r}_{\mathrm{L}}(t))$. The information about the position $\mathbf{r}$ of a particle in D dimensions contained in a scan of the laser position $\mathbf{r}_{\mathrm{L}}(t)$ is quantified by the associated $D\times D$ Fisher information matrix [35], $\mathbf{F}$ which for $p(t_1,\ldots,t_k|\mathbf{r})$ given above has j,k elements given by

$$[\mathbf{F}]_{jk}\equiv F_{jk} = \sum_{K=0}^{\infty}\int_0^\tau dt_1\ldots dt_K\; p(t_1,\ldots,t_K|\mathbf{r})\left(\partial_j\ln\left[p(t_1,\ldots,t_K|\mathbf{x})\right]\right)\left(\partial_k\ln\left[p(t_1,\ldots,t_K|\mathbf{r})\right]\right) \tag{5}$$

where $\partial_j\equiv\partial/\partial r_j$. The Cramér-Rao bound is the statement that the best unbiased estimator of $\mathbf{r}$ has a covariance matrix given by $\mathbf{V}=\mathbf{F}^{-1}$ [35]. Thus, we seek the scan path $\mathbf{r}_{\mathrm{L}}(t)$ that maximizes $\mathbf{F}$ and correspondingly minimizes the covariance $\mathbf{V}$. For one-dimensional estimation, this is a straightforward scalar maximization task, but in higher dimensions we must choose a scalar quantity that characterizes the "size" $\phi[\mathbf{F}]$ of the matrix $\mathbf{F}$. (Below we show that for the 1D case, maximizing $\mathbf{F}$ maximizes the signal to noise ratio. In higher dimensions there is more than one signal and choosing $\phi[\mathbf{F}]$ is equivalent to choosing what function of these signals is to be maximized relative to the noise) Two common choices for quantifying the size of $\mathbf{F}$ are the determinant $\phi_0[\mathbf{F}]=\det[\mathbf{F}]^{1/d}$ and the trace of its inverse $\phi_{-1}[\mathbf{F}]=d\mathrm{Tr}\left[\mathbf{F}^{-1}\right]^{-1}$, which in turn bound the determinant and trace of the covariance matrix $\mathbf{V}$. The trace of the covariance matrix, and hence $\phi_{-1}[\mathbf{F}]$, is particularly important for our case since it is proportional to the localization accuracy (*e.g.* for $D=3$, $\mathrm{Tr}[\mathbf{V}]=\sigma_x^2+\sigma_y^2+\sigma_z^2$). The functions ϕ_0 and ϕ_{-1} are only two examples of the more general matrix information function ϕ_p used in Ref. [36], and defined for all $p\neq 0$ by

$$\phi_p[\mathbf{F}] = \left(\frac{1}{d}\mathrm{Tr}\left[\mathbf{F}^p\right]\right)^{1/p} = \left(\frac{1}{d}\mathrm{Tr}\left[\underbrace{\mathbf{F}\cdot\mathbf{F}\cdot\ldots\cdot\mathbf{F}}_{p\text{ times}}\right]\right)^{1/p} \tag{6}$$

where "$\cdot$" indicates matrix multiplication. These provide a sensible measure of the information content for all $p\leq 1$ [36]. It is important to note that, except in special cases of high symmetry, the optimal scan path maximizing $\phi_p[\mathbf{F}]$ depends on the choice of p as we will show explicitly below for a Gaussian beam in three dimensions.

For any pair of fluorophore coordinates x_j and x_k, a straightforward computation of $\mathbf{F}$ using the above definition yields

$$\begin{aligned} F_{jk} &= \int_0^\tau dt\frac{1}{\Gamma(\mathbf{r}-\mathbf{r}_{\mathrm{L}}(t))}\left(\partial_j\Gamma(\mathbf{r}-\mathbf{r}_{\mathrm{L}}(t))\right)\left(\partial_k\Gamma(\mathbf{r}-\mathbf{r}_{\mathrm{L}}(t))\right) \\ &= 4\int_0^T dt\left(\partial_j\sqrt{\Gamma(\mathbf{r}-\mathbf{r}_{\mathrm{L}}(t))}\right)\left(\partial_k\sqrt{\Gamma(\mathbf{r}-\mathbf{r}_{\mathrm{L}}(t))}\right) \end{aligned} \tag{7}$$

Using $\sqrt{\Gamma(\mathbf{r})} = \sqrt{\xi I(\mathbf{r})} = \sqrt{\xi}\, a(\mathbf{r})$ with $a(\mathbf{r})$ the modulus of the field amplitude we can define

$$\mathbf{g} = 2\nabla\sqrt{\Gamma(\mathbf{r}-\mathbf{r}_{\mathrm{L}}(t))\,\tau} = 2\sqrt{\xi\,\tau}\,\nabla a(\mathbf{r}-\mathbf{r}_{\mathrm{L}}(t))$$

where ∇ is the gradient, i.e., $\nabla_i = \partial_i$. Treating $\mathbf{g}$ as a column vector and indicating the transpose with a superscript T,

$$\mathbf{F} = \frac{1}{\tau}\int_0^\tau dt\ \mathbf{g}\cdot\mathbf{g}^{\mathrm{T}}.$$

If the beam is moved in N discrete steps, dwelling at each position $\mathbf{r}_{\mathrm{L}}^{(n)}$ for a time Δt_n, we can define a vector $\mathbf{g}_n$ for each laser position and write the Fisher information matrix simply a

$$\begin{aligned}\mathbf{F} &= \sum_{n=1}^{N} c_n\,\mathbf{g}_n\cdot\mathbf{g}_n^{\mathrm{T}} \quad , \quad c_n = \Delta t_n/\tau \\ &= 4\xi\sum_{n=1}^{N}\Delta t_n\,\nabla a\left(\mathbf{r}-\mathbf{r}_{\mathrm{L}}^{(n)})\right)\cdot\nabla a\left(\mathbf{r}-\mathbf{r}_{\mathrm{L}}^{(n)})\right)^{\mathrm{T}} \end{aligned} \tag{8}$$

This is the same Fisher information matrix obtained in a classical linear regression model where the unknown particle position $\mathbf{r}$ is projected onto a set of regression vectors $\mathbf{g}_n$ with corresponding weights c_n, with observations corrupted by zero-mean measurement errors of unit magnitude. In this representation, the *length* of a regression vector determines the *precision* of a measurement along that direction. The optimal experimental design problem is to choose a set of N vectors $\mathbf{g}_n$ and corresponding weights c_n - or equivalently, a set of N laser positions $\mathbf{r}_{\mathrm{L}}^{(n)}$ and dwell times Δt_n - that maximizes the information matrix $\mathbf{F}$ relative to the criterion $\phi_p[\mathbf{F}]$.

The theory of optimal experimental design provides a very general and extensive analysis of the solution to this type of problem [36]. For the $\phi_p$optimality criteria defined above an experimental design with associated Fisher matrix $\mathbf{F}_*$ is ϕ_p-optimal if and only if

$$\mathbf{g}^{\mathrm{T}}\cdot\mathbf{F}_*^{p-1}\cdot\mathbf{g} \le \mathrm{Tr}\,[\mathbf{F}_*^p] \tag{9}$$

for *all* possible regression vectors $\mathbf{g}$; in this case all possible scan paths, with equality being achieved only for vectors $\mathbf{g}$ that are part of an optimal scan path. (For a Gaussian beam in 3D this is shown explicitly below in Section 3.2, see in particular Fig 2. We provide a justification for this form of the optimality condition in Appendix A.)

Substituting for $\mathbf{g}$, we can also write that a laser scan path is ϕ_p-optimal for any finite $p \le 1$ if and only if

$$(\nabla a(-\mathbf{r}))^{\mathrm{T}}\cdot\mathbf{F}_*^{p-1}\cdot(\nabla a(-\mathbf{r})) \le \frac{1}{4\xi\,\tau}\mathrm{Tr}\,[\mathbf{F}_*^p] \tag{10}$$

for all $\mathbf{r}$; again, equality is achieved only for $\mathbf{r}$ values that lie on an optimal scan path. Any laser scan path can be tested for optimality by computing the information matrix $\mathbf{F}$ and testing for optimality using this criterion. Unfortunately, although it is reasonably easy to apply, it is not at all obvious how this process yields an optimum scan path. So in order to gain insight into the solution we will first solve the optimization problem by the more conventional approach of using the calculus of variations. This will not only specify the optimum scan path in a obvious way, it will also provide significant insight into the solution including indicating how to alter the intensity distribution Γ to improve the tracking accuracy. We will then show that for the Gaussian beam this yields precisely same result that is found using Eq. 10

3. Solution via the Calculus of Variations

$\mathbf{F}$ is a functional of the laser scan trajectory $\mathbf{r}_{\mathrm{L}}(t)$ and so the optimum trajectory with respect to $\phi_p[\mathbf{F}]$ defined in Eq 6 is the one for which the change in $\phi_p[\mathbf{F}]$ vanishes to first order in $\delta\mathbf{r}_{\mathrm{L}}(t)$ when $\mathbf{r}_L(t) \rightarrow \mathbf{r}_{\mathrm{L}}(t) + \delta\mathbf{r}_{\mathrm{L}}(t)$. Of course this condition only gives an extremum of $\phi_p[\mathbf{F}]$ and we must separately determine that a given solution maximizes $\phi_p[\mathbf{F}]$. Carrying out the variation and setting the result to zero yields

$$0 = \left(\frac{1}{d}\mathrm{Tr}\left[\mathbf{F}^p\right]\right)^{1/p-1}\left[\mathbf{F}^{p-1}\right]_{kj}\left(\partial_k a\left(\mathbf{r}-\mathbf{r}_{\mathrm{L}}(t)\right)\right)\left(\partial_i\partial_j a\left(\mathbf{r}-\mathbf{r}_{\mathrm{L}}(t)\right)\right) \tag{11}$$

with repeated indices, $j,k,\ldots$ summed over the appropriate range and we have used that fact that $\mathbf{F}$ is symmetric. .

In 1 dimension (1D) $\mathbf{F}$ is a non-negative scalar, i.e., $\mathbf{F} = F$ and assuming it does not vanish Eq. 11 reduces to

$$0 = \left(\partial_x a\left(x-x_{\mathrm{L}}(t)\right)\right)\left(\partial_x{}^2 a\left(x-x_{\mathrm{L}}(t)\right)\right)$$

for all p which shows that $\phi_p[\mathbf{F}]$ is maximized at positions $x_L(t)$ where $\partial_x{}^2 a\left(x-x_{\mathrm{L}}(t)\right) = 0$ with $\left|\partial_x a\left(x-x_{\mathrm{L}}(t)\right)\right| \neq 0$. But $\partial_x{}^2 a\left(x-x_{\mathrm{L}}(t)\right) = 0$ is simply the condition that $\left|\partial_x a\left(x-x_{\mathrm{L}}(t)\right)\right|$ is, neglecting inflection points, a maximum. Interestingly this does not correspond to the maximum slope of the intensity itself. Thus we can improve the localization accuracy by maximizing the absolute slope beam amplitude and if there are multiple positions where $\partial_x{}^2 a\left(x-x_{\mathrm{L}}(t)\right) = 0$ then the global optimum is achieved by using the one with the largest value of $\left|\partial_x a\left(x-x_{\mathrm{L}}(t)\right)\right|$. Under the assumption that during the scan time the particle position x is essentially constant it follows that $x_L(t)$ can also be held constant. For a Gaussian beam in 1D [30], $a(x) = a_0 \exp\left[-x^2/w_0^2\right]$ and we have $\partial_x{}^2 a\left(x-x_{\mathrm{L}}\right) = 0$ for $x_{\mathrm{L}} = x \pm w_0/\sqrt{2}$ with both solutions having the same value of $|\partial_x a|$. $\phi_p[\mathbf{F}]$ is therefore a maximum for $F = F_* = 8\xi\tau a_0{}^2/\left(ew_0{}^2\right) = 8N_{ph}/\left(ew_0{}^2\right)$ .where $N_{ph} = \xi\tau a_0{}^2/e$ is the mean number of photons collected during the scan. Obviously $\left|\partial_x a(x)\right|$ needs to maintain a large value over the range of uncertainty in the particle position Δx, i.e., $\left|\partial_x a\left(x-\varepsilon\Delta x-x_{\mathrm{L}}\right)\right|$ should be approximately constant, and large, for $-1 \lesssim \varepsilon \lesssim +1$.

Next consider the 1D case from the point of view of the intensity rather than the amplitude, i.e., from the point of view of the first line of Eq. 7. In this form F is maximized at positions where the slope of the intensity, $\partial_x I$, is a maximum with the intensity I itself being a minimum. At first requiring I to be a minimum seems counterintuitive. But the signal amplitude is on the order of $\partial_x I \times \Delta x$ while the absolute noise level is proportional to $\sqrt{I}$ and so the signal to noise ratio for a given Δx is maximized at positions where $\left|(\partial_x I)\right|/\sqrt{I}$ or equivalently $(\partial_x I)^2/I$ is a maximum. Hence maximizing F in 1D is equivalent to maximizing the signal to noise ratio.

This 1D solution generalizes directly to 2D and 3D. Eq 11 can be satisfied by choosing positions that have $\partial_i\partial_j a(\mathbf{r}) = 0$ for all i and j. Again the beam can be held stationary at a sufficient number of these positions during the scan time although a continuous trajectory which maintains these conditions may be easier to implement mechanically and/or optically. The condition $\partial_i\partial_j a(\mathbf{r}) = 0$ for $i = j$ is exactly the same as the condition $\partial^2 a(x) = 0$ in 1D. For $i \neq j$ this condition effectively amounts to having the gradients of $a(\mathbf{r})$ at the chosen positions be mutually orthogonal But, as opposed to 1D where the entire measurement time τ can be spent with the beam locked at one position, in 2D and 3D it is not immediately clear how to divide up the time among the different positions. To be specific let the positions which maximize $\phi_p[\mathbf{F}]$ be $\mathbf{r}_L^{(s)}$, with s ranging from 1 to D where D is the number of dimensions and assume that ∇a at each point separately aligns with one of the coordinate axes so that $\nabla a\left(\mathbf{r}-\mathbf{r}_{\mathrm{L}}^{(s)}\right)$ points purely

in the r_s direction, i.e., $\nabla a\left(\mathbf{r}-\mathbf{r}_{\mathrm{L}}^{(1)}\right)$ points purely in the x direction, and so on, then

$$\phi_p[\mathbf{F}] = \left(\frac{1}{D}\sum_{s=1}^{D}\Delta t_s{}^p\left|\partial_s a\left(\mathbf{r}-\mathbf{r}_{\mathrm{L}}^{(s)}\right)\right|^{2p}\right)^{1/p} \tag{12}$$

with the constraint that $\sum_{s=1}^{D}\Delta t_s = \tau$. Invoking the constraint by setting $\Delta t_D = \tau - \sum_{s=1}^{D-1}\Delta t_s$ the dwell times Δt_p at each position can be chosen by solving

$$\frac{\partial\phi_p[\mathbf{F}]}{\partial(\Delta t_s)} = 0 \text{ for } s = 1 \text{ to } D-1$$

Note that if the values of $\left|\partial_s a\left(\mathbf{r}-\mathbf{r}_{\mathrm{L}}^{(s)}\right)\right|$ are the same at all the laser positions then this directly yields that the Δt_s are equal to τ/D independent of the value of p.

We now apply this solution technique in 3D to a Gaussian beam which has a field amplitude given by [30]

$$a(x,y,z) = \frac{a_0}{\sqrt{1+z^2/z_{\mathrm{R}}^2}}\exp\left[-\frac{1}{w_0^2}\left(\frac{x^2+y^2}{1+z^2/z_{\mathrm{R}}^2}\right)\right]$$

where $z_{\mathrm{R}} = \pi {w_0}^2/\lambda$ is the Rayleigh range, λ is the wavelength and $a_0 = \sqrt{I_0}$. Assume the particle position $\mathbf{r}$ is approximately zero on the scale of the width of the Gaussian. Then the positions of center of the Gaussian beam that have the maximum slope in each of the x,y and z directions at the origin are $\mathbf{r}_{\mathrm{L}}^{(1)} = \left(\pm w_0/\sqrt{2},0,0\right)$, $\mathbf{r}_{\mathrm{L}}^{(2)} = \left(0,\pm w_0/\sqrt{2},0\right)$,as before and $\mathbf{r}_{\mathrm{L}}^{(3)} = \left(0,0,\pm z_{\mathrm{R}}/\sqrt{2}\right)$. For 2D localization the symmetry of the Gaussian in the xy plane Eq. 12 yields dwell times at $\mathbf{r}_{\mathrm{L}}^{(1)} = \left(\pm w_0/\sqrt{2},0,0\right)$ and $\mathbf{r}_{\mathrm{L}}^{(2)} = \left(0,\pm w_0/\sqrt{2},0\right)$ which are both equal to $\tau/2$.. For localization in all three directions the difference between the slope in the z direction and those in the x and y directions causes the dwell times to depend on p. For $p=-1$ Eq. 12 we get

$$\begin{aligned}\Delta t_1 &= \Delta t_2 = \frac{w_0\tau}{2w_0+9z_{\mathrm{R}}/\sqrt{6e}}\\ \Delta t_3 &= \frac{\left(9z_{\mathrm{R}}/\sqrt{6e}\right)\tau}{2w_0+9z_{\mathrm{R}}/\sqrt{6e}}\end{aligned}$$

whereas for $p=0$ we get $\Delta t_1 = \Delta t_2 = \Delta t_3 = \tau/3$.

In both 2D and 3D the $\pm$ signs lead to minor ambiguity in the particle position since nominally one cannot tell which side of the beam the particle is on. In many cases only the movement of the particle relative to it's starting position is required and so the absolute position is not required. But the ambiguity can be lifted in any case simply by dithering the beam position slightly in each direction and determining the sign of the change in signal level.

In the next section we show that the 2D solution for arbitrary p and the 3D solution for $p=-1$ derived here are exactly the same as those given by Eq. 10

3.1. Gaussian Beam in Two Dimensions via Optimal Design

In the two-dimensional case, the experimental design problem is straightforward. The beam geometry assuming the particle is maintained at the beam waist $(z=0)$ is $\Gamma(\mathbf{r}) = \Gamma(x,y) = \Gamma_0\exp\left[-\frac{2}{w_0^2}(x^2+y^2)\right]$ withe $\Gamma_0 = \xi I_0 = \xi {a_0}^2$with I_0 the peak intensity in terms of the number

of photons/(area $\times$ time) [30]. When this beam is offset by a position shift of $\mathbf{r} = (x,y)$ from the origin the regression vector $\mathbf{g}$ is given by

$$\mathbf{g} = \frac{4\mathbf{r}}{w_0^2}\sqrt{\Gamma(-\mathbf{r})\tau}.$$

Scanning at the two (x,y) positions $\mathbf{r}_{\mathrm{L}}^{(1)} = (w_0/\sqrt{2},0)$ and $\mathbf{r}_{\mathrm{L}}^{(2)} = (0,w_0/\sqrt{2})$ as determined in the previous section for equal times $\Delta t_1 = \Delta t_2 = \tau/2$, we find the Fisher information matrix

$$\mathbf{F}_* = \frac{4}{w_0^2}\frac{\Gamma_0\tau}{e}\begin{pmatrix}1 & 0\\ 0 & 1\end{pmatrix} = \frac{4N_{ph}}{w_0^2}\begin{pmatrix}1 & 0\\ 0 & 1\end{pmatrix}$$

where the (mean) number of photons collected during a single scan period is $N_{ph} = \Delta t_1\Gamma(\mathbf{r}_1) + \Delta t_2\Gamma(\mathbf{r}_2) = \Gamma_0\tau/e = \xi {a_0}^2\tau/e$.

Note that the same Fisher matrix is achieved for any pair of orthogonal vectors or for a constant-speed circular scan about the origin so long as the scan points lie on the circle with radius $r = w_0/\sqrt{2}$ [26].

For any other laser focal position $\mathbf{r}'$, the optimality inequality Eq. 10 for any finite $p \le 1$ becomes

$$(x'^2 + y'^2)e^{-\frac{2}{w_0^2}(x'^2+y'^2)} \overset{?}{\le} \frac{w_0^2}{2e},$$

which is satisfied for all $\mathbf{r}' = (x',y')$. The Cramér-Rao bound on the two-dimensional localization accuracy corresponding to $p = -1$ becomes $\sigma_x^2 + \sigma_y^2 \ge \mathrm{Tr}(\mathbf{F}_*^{-1})$, so that

$$\sigma_x^2 + \sigma_y^2 \ge \frac{w_0^2}{2N_{ph}}$$

as quoted in Eq. 1. Note that due to the symmetry of the Gaussian in 2D this result is independent of p.

3.2. Gaussian Beam in Three Dimensions via Optimal Design

The situation is more complex in three dimensions. Consider the beam profile given by the usual expression [30]

$$\Gamma(\mathbf{r}) = \Gamma(x,y,z) = \frac{\Gamma_0}{1+z^2/z_{\mathrm{R}}^2}\exp\left[-\frac{2}{w_0^2}\left(\frac{x^2+y^2}{1+z^2/z_{\mathrm{R}}^2}\right)\right].$$

Here, ϕ_0 and ϕ_{-1} optimality are *not* achieved by the same scan path, so we focus on ϕ_{-1}, which bounds the localization accuracy $\sigma_x^2 + \sigma_y^2 + \sigma_z^2$. We can determine optimality by testing a candidate solution. We show that the optimal path is the one derived above given by

$$\mathbf{r}_{\mathrm{L}}^{(1)} = \left(\pm\frac{w_0}{\sqrt{2}}\ ,\ 0\ ,\ 0\right) \qquad \Delta t_1 = \frac{w_0\tau}{2w_0 + 9z_{\mathrm{R}}/\sqrt{6e}} \tag{13a}$$

$$\mathbf{r}_{\mathrm{L}}^{(2)} = \left(0\ ,\ \pm\frac{w_0}{\sqrt{2}}\ ,\ 0\right) \qquad \Delta t_1 = \frac{w_0\tau}{2w_0 + 9z_{\mathrm{R}}/\sqrt{6e}} \tag{13b}$$

$$\mathbf{r}_{\mathrm{L}}^{(3)} = \left(0\ ,\ 0\ ,\ \pm\frac{z_{\mathrm{R}}}{\sqrt{2}}\right) \qquad \Delta t_3 = \frac{\left(9z_{\mathrm{R}}/\sqrt{6e}\right)\tau}{2w_0 + 9z_{\mathrm{R}}/\sqrt{6e}}. \tag{13c}$$

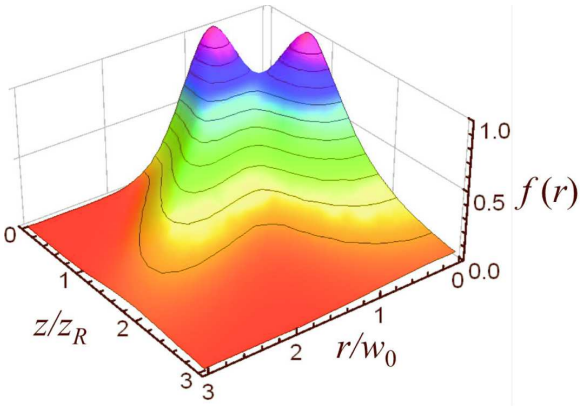

Fig. 2. Plot of $f(\mathbf{r})$ as defined in Eq.14. The scan path given by Eqs. (13a-13c) are proved to be optimal by observing that $f(\mathbf{r})$ is less than1 for all other values of r/w_0 or z/z_R. Note that because the two optimal points, i.e., the peaks in the graph in Fig. 2, are separated by a valley ($f<1$) there is no smoothly varying continuous path in 3D that is optimal for a Gaussian beam. This is in contrast to the 2D case with a Gaussian beam where all the points on the circle $r=w_0/\sqrt{2}$ have $f=1$ and hence a continuous path can be used if desired. [26].

The Fisher matrix for this scan path, $\mathbf{F}_*$, is diagonal and is given by

$$\begin{aligned}\mathbf{F}_{*11} &= \mathbf{F}_{*22}=\frac{8\Gamma_0\tau/e}{2w_0^2+9z_{\mathrm{R}}/\sqrt{6e}}\approx\frac{\Gamma_0\tau}{0.68w_0^2+0.76w_0z_{\mathrm{R}}}\\ \mathbf{F}_{*33} &= \frac{16\Gamma_0\tau/\sqrt{6e}}{6w_0z_R+27z_{\mathrm{R}}^2/\sqrt{6e}}\approx\frac{\Gamma_0\tau}{1.51w_0z_R+1.69z_{\mathrm{R}}^2}\end{aligned}$$

To prove the optimality of this path, we compute the following test function [*c.f.* Eqs. 9 and 10 with $p=-1$]:

$$f(\mathbf{r})=\frac{\mathbf{g}^{\mathrm{T}}\cdot\mathbf{F}_*^{-2}\cdot\mathbf{g}}{\mathrm{Tr}\left[\mathbf{F}_*^{-1}\right]}=4\xi\tau\frac{(\nabla a(-\mathbf{r}))^{\mathrm{T}}\mathbf{F}_*^{-2}(\nabla a(-\mathbf{r}))}{\mathrm{Tr}\left[\mathbf{F}_*^{-1}\right]}. \tag{14}$$

According to the optimality criteria, the scan path is optimal if and only if $f(\mathbf{r})\le 1$ for all $\mathbf{r}$. Writing $\mathbf{r}=(x,y,z)$ in convenient dimensionless units where $r=\sqrt{x^2+y^2}$, $\bar{r}=r/w_0$ and $\bar{z}=z/z_R$ we find

$$f(\mathbf{r})=\frac{8e\bar{r}^2(1+\bar{z}^2)^2+27\bar{z}^2(1-2\bar{r}^2+\bar{z}^2)^2}{4(1+\bar{z}^2)^5}\exp\left[-\frac{2\bar{r}^2}{1+\bar{z}^2}\right]. \tag{15}$$

This function is plotted in Fig.2, where it is clearly seen not to exceed the value 1 (this can also be shown analytically). Thus, the proposed scan path is ϕ_{-1}-optimal and therefore the three-dimensional localization is always limited by the Cramér-Rao bound, taking here the form

$$\sigma_x^2+\sigma_y^2+\sigma_z^2\ge\mathrm{Tr}\left[\mathbf{F}_*^{-1}\right].$$

Note that because the two optimal points, i.e., the peaks in the graph in Fig. 2, are separated by a valley ($f<1$) there is no smoothly varying continuous path in 3D that is optimal for a Gaussian beam. This is in contrast to the 2D case with a Gaussian beam where all the points

on the circle $r = w_0/\sqrt{2}$ have $f = 1$ and hence a continuous path can be used if desired. [26] The fact that no smoothly varying continuous path is possible in 3D has obvious implications with respect to the practical implementation of these results. True optimality requires the beam to hop instantaneously between $z = 0$ with $r = w_0/\sqrt{2}$ and $r = 0$ with $z = z_R/\sqrt{2}$. In a strict sense this is not possible physically but obviously any system with a hopping time which is tiny fraction of τ will for all practical purposes be optimal.

Computing the number of photons collected along the scan path during a single period from $N_{ph} = \sum_{k=1}^{3} \Gamma(\mathbf{r}_k)\Delta t_k$, we can rewrite the best possible three-dimensional localization accuracy, achieved for the optimal scan path given by the weighted solution as

$$\sigma_x^2 + \sigma_y^2 + \sigma_z^2 \geq \frac{w_0^2}{2N_{ph}} \left[1 + \sqrt{\frac{3}{2}} \left(\sqrt{e} + \frac{3}{2\sqrt{e}} \right) \frac{z_R}{w_0} + \frac{9}{4} \frac{z_R^2}{w_0^2} \right].$$

Plugging in the standard expression $z_R = \pi w_0^2/\lambda$ [30], we recover Eq. 2, proving the initial claim.

4. Conclusions

We have used the calculus of variations to derive the optimum scan path for tracking and localizing a fluorescent particle and have shown that for Gaussian beams in two and three dimensions the calculus of variations result matches the solution derived from the optimal design of experiments. In one dimension this condition corresponds simply to maximizing the signal to noise ratio. In higher dimensions there are multiple signals, essentially one for each direction, and depending on how these are combined into a single signal there are different optimization criteria which is equivalent to having to choose the value of p in the merit function $\phi_p[\mathbf{F}]$. These results provide a simple, testable optimality criterion to determine whether a candidate laser scan path encodes maximal information about a fluorescent particles position in the detected photon stream. We presented optimal scan paths for two- and three-dimensional Gaussian beams and used these to derive the best possible localization accuracies, quoted in the introduction. We have shown that the optimal path for 2D localization using a Gaussian beam can be continuous if desired, but the optimal path in 3D for a Gaussian cannot be continuous. These results can be applied to other experimental geometries, including those where multiple detectors - rather than multiple beam positions - are used for real-time localization. Future work should focus on relaxing the assumption that the particle remains effectively stationary during each scan cycle so as to extend optimality results to cases where the particle is moving under a particular dynamic model (for example, free diffusion or diffusion plus flow) or where feedback control may not be sufficiently tight that the particle is well-localized relative to the beam size. Also, it would be worthwhile to determine if there are physically realizable intensity distributions which do allow for the optimal path to be continuous as this might aid the practical implementation of these results.

5. Appendix A: Justification of the Global Optimality Criterion

The rigorous proof of the optimality condition Eq. 9 is rather complex and will not be presented here. Instead we will present a justification for it. By definition $\mathbf{F}_*$ is ϕ_p optimal relative to all other $\mathbf{F}$ if and only if

$$\phi_p[\mathbf{F}] \leq \phi_p[\mathbf{F}_*]$$

Substituting the definition of ϕ_p from Eq. 6 into the above condition, raising both sides to the power p and cancelling factors of $1/d$ gives

$$\mathrm{Tr}[\mathbf{F}^p] \leq \mathrm{Tr}[\mathbf{F}_*^p]$$

Writing $\mathrm{Tr}\left[\mathbf{F}_*^p\right] = \left(\mathbf{F}_*^{p-1}\right)_{ij}[\mathbf{F}_*]_{ji}$, using $[\mathbf{F}_*]_{ji} = F_{*ji} = \sum_{n=1}^{N} g_{*nj}g_{*ni}$ after absorbing the c_n into the definition of the $\mathbf{g}_n$ and rearranging gives

$$\mathrm{Tr}\left[\mathbf{F}_*^p\right] = \sum_{n=1}^{N} g_{*ni}\left[\mathbf{F}_*^{p-1}\right]_{ij} g_{*nj} = \sum_{n=1}^{N} \mathbf{g}_{*n}^{\mathrm{T}} \cdot \mathbf{F}_*^{p-1} \cdot \mathbf{g}_{*n}$$

All $\mathbf{F}$ are real and symmetric and so can be diagonalized by a similarity transformation. Let the similarity transformation which diagonalizes $\mathbf{F}_*$ be $\mathbf{S}$ whose rows are the orthonormal eigenvectors $\mathbf{e}_i$ of $\mathbf{F}_*$ with $i = 1, \ldots, D$ in D dimensions. Then $\mathbf{S} \cdot \mathbf{F}_* \cdot \mathbf{S}^{\mathrm{T}} = \mathbf{f}_*$ is diagonal and $\mathbf{S}^{\mathrm{T}} \cdot \mathbf{S}$ is the identity matrix. The diagonal elements of $\mathbf{f}_*$ given by f_{*i} are real and positive since

$$\mathbf{v}^{\mathrm{T}} \cdot \mathbf{F}_* \cdot \mathbf{v} = \sum_{n=1}^{N} \left(v_i g_{*ni}\right)^2 > 0$$

for any real nonzero $\mathbf{v}$. Writing $\mathbf{g}_{*n}$ in terms of the eigenvectors $\mathbf{e}_i$ (written as column vectors) gives

$$\mathbf{g}_{*n} = \sum_{i=1}^{D} \bar{g}_{*ni}\mathbf{e}_i$$

As we have seen above, in D dimensions we only need D independent measurements to determine the particles position, i.e., $N = D$, and that in the representation where $\mathbf{F}$ is diagonal that these optimum positions are orthogonal to one another which means

$$\bar{g}_{*ni} = \bar{g}_{*i}\delta_{n,i}$$

Substituting this into $\mathbf{S} \cdot \mathbf{F}_* \cdot \mathbf{S}^{\mathrm{T}} = \mathbf{f}_*$ we find

$$\sum_{n=1}^{N} \bar{g}_{*ni}\bar{g}_{*nj} = \bar{g}_{*i}\bar{g}_{*j}\delta_{ij} = \mathrm{f}_{*i}\delta_{ij}$$

with no sum on i.or j which gives $\bar{g}_{*i} = \sqrt{\mathrm{f}_{*i}}$and

$$\sum_{n=1}^{N} \mathbf{g}_{*n}^{\mathrm{T}} \cdot \mathbf{f}_*^{p-1} \cdot \mathbf{g}_{*n} = \mathbf{g}_*^{\mathrm{T}} \cdot \mathbf{f}_*^{p-1} \cdot \mathbf{g}_*$$

If we now replace $\mathbf{g}_*$ with an arbitrary $\mathbf{g}$ and undo the similarity transformation we have by definition

$$\mathbf{g}^{\mathrm{T}} \cdot \mathbf{F}_*^{p-1} \cdot \mathbf{g} \leq \mathrm{Tr}\left[\mathbf{F}_*^p\right]$$

Appendix B: Maximum Likelihood Position Estimation for an Arbitrary Scan Path

In earlier sections, we derived design criteria for determining which laser scan path contains the most information about a particle's position, when the particle is near the origin of coordinates. In general, however, we also require an estimation procedure that can extract the position from the detected photon stream. This position estimator must, of course, include some information about the beam size, shape, and the scan path. One candidate is a maximum likelihood estimator, whose performance will be uncertain when the photon number is very small but will tend towards optimality for large photon numbers (how large cannot be determined *a priori* and is a common criticism of maximum likelihood). In this appendix, we derive a simple linear form for the maximum likelihood estimator of a fluorescent particle's position for an arbitrary (2D

or 3D) scan path, under the assumption that the particle position $\mathbf{r}$ is close to the origin. To do this, we can expand the time-detection rate function to second order in $\mathbf{r}$ as

$$\Gamma[\mathbf{r}-\mathbf{r}_{\mathrm{L}}(t)] \approx \Gamma[-\mathbf{r}_L(t)] + \mathbf{r}^T\,\nabla\Gamma|_{-\mathbf{r}_L(t)} + \frac{1}{2}\mathbf{r}^T\,\mathbf{H}(\Gamma)|_{-\mathbf{r}_L(t)}\,\mathbf{r} + O(\mathbf{r}^3) \tag{16}$$

where $\mathbf{H}(\Gamma)|_{-\mathbf{r}_{\mathrm{L}}(t)}$ is the Hessian matrix of partial derivatives of the laser intensity function evaluated at the point $-\mathbf{r}_{\mathrm{L}}(t)$. For any function $f(\mathbf{r})$, the jk entry of the Hessian matrix is $[\mathbf{H}(f)]_{jk} = \frac{\partial^2 f}{\partial x_j \partial x_k}$. Plugging this second-order approximation into the likelihood function of Eq. 4 and setting the gradient with respect to particle position $\mathbf{r}$ to zero, we find the following linear equation for the *maximum likelihood estimate* $\mathbf{r}_{\mathrm{MLE}}$ of the particle position $\mathbf{r}$:

$$\mathbf{A}\mathbf{r}_{\mathrm{MLE}} + \mathbf{b} = \mathbf{0} \tag{17a}$$

where the $D\times D$ matrix $\mathbf{A}$ and $D\times 1$ vector $\mathbf{b}$ depend on the laser scan path and the measurement result $\{t_1,\ldots,t_k\}$ through

$$\mathbf{A} = -\int_0^\tau \mathbf{H}(\Gamma)|_{-\mathbf{r}_{\mathrm{L}}(t)}\,\mathrm{d}t + \sum_{k=1}^{K} \mathbf{H}(\log\Gamma)|_{-\mathbf{r}_{\mathrm{L}}(t_k)} \tag{17b}$$

$$\mathbf{b} = -\int_0^\tau \nabla(\Gamma)|_{-\mathbf{r}_{\mathrm{L}}(t)}\,\mathrm{d}t + \sum_{k=1}^{K} \nabla(\log\Gamma)|_{-\mathbf{r}_{\mathrm{L}}(t_k)}\,. \tag{17c}$$

The sums over k are understood to be 0 when $K=0$. When the functional form of the terms in $\mathbf{A}$ and $\mathbf{b}$ can be precomputed or approximated, a real-time position estimate can be formed by computing $\mathbf{A}$ and $\mathbf{b}$ in real time (through the sums over k) and solving the 2- or 3-dimensional linear system.

As a simple example, consider the two-dimensional Gaussian beam example of Sect. with the circular scan path $\mathbf{r}_{\mathrm{L}}(t) = \frac{w}{\sqrt{2}}(\cos\frac{2\pi t}{\tau}, \sin\frac{2\pi t}{\tau})^{\mathrm{T}}$. By direct computation, we find

$$\mathbf{A} = -K\begin{pmatrix}1 & 0\\ 0 & 1\end{pmatrix} \quad , \quad \mathbf{b} = \frac{w}{\sqrt{2}}\sum_{k=1}^{K}\mathbf{r}_{\mathrm{L}}(t_k) \tag{18}$$

so that

$$\mathbf{r}_{\mathrm{MLE}} = \begin{cases} \mathbf{0} & , \quad K=0 \\ \frac{w}{\sqrt{2}}\left(\frac{1}{K}\sum\limits_{k=1}^{K}\cos\frac{2\pi t_k}{\tau}, \frac{1}{K}\sum\limits_{k=1}^{K}\sin\frac{2\pi t_k}{\tau}\right)^{\mathrm{T}} & , \quad K>0 \end{cases} \tag{19}$$

Note that the maximum likelihood estimate for this case is given by phase-sensitive lock-in detection of the photon stream t_k [26].